Journal of Applied Polymer Science

Preparation and properties of crosslinked network coatings based on perfluoropolyether/poly(dimethyl siloxane)/acrylic polyols for marine fouling-release applications

Xiaoying Sun,[1*] Fan Zhang,[1*] Yuanyuan Chen,[2] Zhang Cheng,[1] Youquan Su,[1] Jianzhong Hang,[1] Lujiang Jin,[1] Na Li,[1] Dan Shang,[1] Liyi Shi[1]

[1]Nanoscience and Technology Center, Shanghai University, Shanghai 200444, People's Republic of China

[2]School of Life Sciences, Shanghai University, Shanghai 200444, People's Republic of China

X. Sun and F. Zhang contributed equally to this article.

Correspondence to: X. Sun (E-mail: xysun@shu.edu.cn)

ABSTRACT: α,ω-Triethoxysilane terminated poly(dimethyl siloxane) (PDMS) oligomer, α,ω-triethoxysilane terminated perfluoropolyether (PFPE) oligomer, and acrylic polyols were first synthesized via an addition reaction and free-radical polymerization. Then, crosslinked network coatings based on PFPE/PDMS/acrylic polyols for marine fouling-release applications were prepared by a condensation reaction. The structure of the crosslinked network coating was characterized by Fourier transform infrared spectroscopy. The chemical composition of the coating surface was characterized by X-ray photoelectron spectroscopy. The thermal properties, surface energy, mechanical properties, adhesion, and antiseawater immersion performance of the coatings were systematically studied. The antibiofouling properties of the crosslinked network coating were evaluated by laboratory biofouling assays with the bacteria *Escherichia coli* and the fouling diatom *Navicula*. The results from the preliminary study suggested that this crosslinked network coating had good adhesion and promising antifouling properties that were comparable to a silicone standard. © 2015 Wiley Periodicals, Inc. J. Appl. Polym. Sci. **2015**, *132*, 41860.

KEYWORDS: addition polymerization; biomaterials; coatings; crosslinking

Received 31 July 2014; accepted 2 December 2014
DOI: 10.1002/app.41860

INTRODUCTION

It is well known that the biofouling of ship hulls by marine organisms (e.g., bacteria, algae, unicellular eukaryotes, e.g., diatoms and invertebrates) will result in lower operational speeds, increased fuel consumption, and higher maintenance costs.[1–3] Traditional biocidal antifouling paints with tributyltin, cuprous oxide, and organic cobiocides as actives have been used to prevent biofouling. However, those actives will be leaked out; these will adversely affect the marine environment.[4] Therefore, the development of nontoxic, environmentally friendly antifouling coatings is being urgently pursued.

The most promising alternative to traditional biocidal antifouling coatings is fouling-release coatings (FRCs). The working mechanism of FRCs is the minimization of the adhesion between fouling organisms and the surface to remove the fouling by hydrodynamic forces during navigation or gentle mechanical cleaning.[5,6] To achieve good fouling-release properties, the coatings should possess a relatively low surface free energy, low elastic modulus, low surface roughness, and so on.[7]

Silicone-based and fluorinated polymers have been considered the most promising candidate matrices for nontoxic FRCs. Silicone-based FRCs with a low surface energy and low modulus are good at preventing fouling organisms, especially macrofoulers, including barnacle adhesion.[8] However, silicones have some disadvantages. First, the typical surface energy of the silicones at 20–24 mJ/m^2 is marginally low enough for an effective release coating. Second, hydrophilic sites migrate to the surface of the silicone coatings to decrease the coating hydrophobicity. Third, silicone-based coatings are typically relatively soft and, therefore, can be easily damaged, and this limits their practical use. Finally, the silicone oil incorporated in silicone-based FRCs may cause marine pollution by leaching into the water.[9–11]

To overcome the pitfall of silicone-based FRCs, people have synthesized polymers that incorporate both siloxane and fluorinated moieties; this couples the low-modulus character of siloxanes with the low surface tension and rigid character of fluorinated polymers.[12–19] Marabotti's group[17] reported the preparation of fluorinated/siloxane copolymers by the reaction of two

commercially available acrylic monomers containing fluorine and silicon, respectively. Then, the FRCs were fabricated by the incorporation of the fluorinated/siloxane copolymers into a PDMS matrix. The results show that the fouling-release properties of the coatings were improved with the use of two important macrofouling organisms, the green alga *Ulva linza* and the barnacle *Balanus amphitrite,* thanks to the stable hydrophobic surface with lower energy surface. Mera and Wynne[18] patented FRCs based on fluorinated silicone and nonfluorinated organopolysiloxane resin. It was disclosed that the surface energies of fluorinated silicone coatings were lower than those of pure silicone FRCs. With the increasing content of fluorine in the network, the surface energy was decreased. Thus, the antifouling performance of the fluorosilicone, especially for barnacles, was better than the PDMS alone. In our previous work,[19] we synthesized acrylic resins containing fluorine/silicone side chain by solution copolymerization with monomethacryloxyalkyl-terminated PDMS, 1H,1H,7H-dodecafluoroheptyl methacrylate, methyl methacrylate (MMA), *n*-butyl acrylate (BA), *n*-butyl methacrylate, and ethyl acrylate as the comonomers. Because of the lower surface energy, the as-prepared fluorine/silicone-modified acrylic resins had better antibiofouling properties than the fluorine- or silicone-modified acrylic resins. Although fluorinated-silicone-based FRCs demonstrated a lower surface energy and good coating rigidity, the adhesion of such coatings on the substrate was very weak.

In this study, novel crosslinked network coatings based on perfluoropolyether (PFPE)/PDMS/acrylic polyols for marine fouling–release applications were prepared. The introduction of siloxane functional groups to the coating further improved the adhesion force to the substrate without comprising the low surface energy of the coating. The surface free energy, thermal stability, mechanical properties, and antifouling properties of the coatings were thoroughly investigated.

EXPERIMENTAL

Materials

Hydroxyethyl methyl acrylate (HEMA) and dibutyltin dilaurate (DBTDL) were purchased from Tokyo Chemical Industry Co, Ltd. Hydroxyl silicone oil (weight-average molecular weight = 1500 g/mol) and standard PDMS resin (DC 3140) were received from Dow Corning. Perfluoropolyether diol (Fluorolink E10-H) was provided by Solvay Solexis. 3-Isocyanatopropyltriethoxysilane was purchased from Diamond Advanced Material of Chemical, Inc. *Escherichia coli* (from China Center of Industrial Culture Collection) and *Navicula* diatoms (from Freshwater Algae Culture Collection at the Institute of Hydrobiology) were used for biofouling assays. All of the other reagents were purchased from Sinopharm Chemical Reagent Co, Ltd.

Oligomer Synthesis

Synthesis of Acrylic Polyols. A mixture of xylene (20 g) and *n*-butyl acetate (20 g) as a solvent was stirred at 85°C. A reaction mixture of BA (50 g), MMA (40 g), HEMA (10 g), and 2,2′-azobisisobutyronitrile (AIBN; 1.6 g) dissolved in xylene (20 g) and *n*-butyl acetate (20 g) was added dropwise to the solvent. After it was stirred for 2 h at 85°C, the reaction mixture was heated to 110°C. A mixture of AIBN (0.4 g) dissolved in xylene (20 g) and *n*-butyl acetate (20 g) was slowly added and stirred for another 2 h. The resulting acrylic polyols, labeled as AOH, appeared as a yellow oil.

Table I. Formulations of the Crosslinked Network Coatings

Sample	PFU (wt %)	TSU (wt %)	AOH (wt %)
TFS-AOH-A1	2	14	84
TFS-AOH-A2	6	10	84
TFS-AOH-A3	10	6	84
TFS-AOH-A4	14	2	84
TFS-AOH-B1	2	2	96
TFS-AOH-B2	4	4	92
TFS-AOH-B3	6	6	88
TFS-AOH-B4	8	8	84
TFS-AOH-B5	10	10	80

Synthesis of α,ω-Triethoxysilane Terminated PFPE Oligomer. 3-Isocyanatopropyltriethoxysilane (5.1870 g) and DBTDL (0.0063 g) were added dropwise to a mixture of Fluorolink E10-H (7.5000 g) and tetrahydrofuran (12.6870 g) and stirred for 2 h at 65°C. The molar ratio of 3-isocyanatopropyltriethoxysilane to Fluorolink E10-H was 2.1:1. The progress of the reaction was monitored with Fourier transform infrared (FTIR) spectrometry by the disappearance of the IR absorption peaks of the isocyanate groups (at ca. 2272 cm^{-1}) and the appearance of the urethane carbonyl related peak at 1720 cm^{-1}. The as-prepared α,ω-triethoxysilane terminated PFPE oligomer was labeled as PFU.

Synthesis of the α,ω-Triethoxysilane Terminated PDMS Oligomer. 3-Isocyanatopropyltriethoxysilane (5.1870 g) and DBTDL (0.0063 g) were slowly added to a mixture of hydroxyl silicone oil (15 g) and tetrahydrofuran (15.1870 g) and stirred for 5 h at 65°C. The progress of the reaction was monitored with FTIR spectrometer as described previously. The resulting α,ω-triethoxysilane terminated PDMS oligomer was labeled as TSU.

Coating Preparation

The as-prepared oligomers, PFU and TSU, were mixed with the acrylic polyol AOH at different concentrations, as shown in Table I. Then, the mixtures were stirred constantly for a further 2 h at room temperature to obtain the coating material.

Glass slides were ultrasonically cleaned in acetone for 15 min and rinsed with deionized water. The as-prepared coating material was cast on glass slides with a 120-μm wire-gauged bar applicator and then placed into an enclosed drying cabinet with ventilation overnight. Furthermore, the coatings were cured at 90°C for 6 h. For biofouling assays, DC 3140 coated slides prepared according to the above process played a role as the reference sample.

Characterization

IR spectra were obtained on Thermo Fisher Corp. Nicoq 380 FTIR spectrometer. The chemical composition of the coating surface was characterized by X-ray photoelectron spectroscopy (XPS; PHI5000C ESCA system) with an AlKα X-ray source. The Al anode voltage was 14 keV, and the power was 250 W. The pressure in the spectrometer during analysis was typically in the

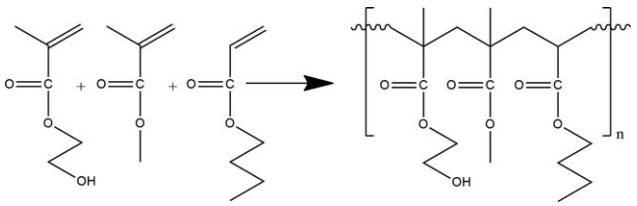

Scheme 1. Reaction scheme for the synthesis of the acrylic polyols.

10^{-8} Torr range. XPS spectra were recorded automatically at a photoemission angle of 54°.

Differential scanning calorimetry (DSC) was used to measure the glass-transition temperature of the polymer and coating materials. DSC was performed on a TA Q500 HiRes differential scanning calorimeter. The samples were heated from −70 to 200°C at the heating rate of 10°C/min.

The contact angles (θs) for water and methylene iodide (MI) were measured with an optical θ meter (Kruss Co. DSA100) at room temperature. Five drops of liquid at different locations in a coated sample were used to measure θs. The average value was taken as θ of the coated sample surface. From each θ measurements, the surface energies were calculated according to the Owens–Wendt method.[20] The elasticity modulus was measured by a Situ Nano Tester (TRIBO INDENTER).

The cross-cut adhesion test was applied according to ASTM D 3359 to evaluate the adhesion of the coating on the substrate. The adhesion could be classified from 5B (good adhesion) to 0B (poor adhesion). The antiseawater immersion performance of the coatings was measured by the placement of the coated samples in artificial seawater, and a change in the sample surface was observed after 21 days.

Biofouling Assays

Bacterial Attachment Experiment. *E. coli* were used for the cell adhesion test according to the literature.[21] The coated sample was exposed to the 30-mL suspension of *E. coli*. After 48 h, the coated sample was taken out from the suspension and was then stained with crystal violet dye for 15 min. With rinsing three times by physiological saline, the sample was imaged with an optical microscope (Leica DM 2500M).

Diatom *Navicula* Settlement Experiment. The diatom *Navicula* was cultivated in a light incubator at 25°C with a light intensity of 2000 Lux for 20 days. The coated samples were incubated at about 25°C for 2 days in a tank of recirculating deionized water. Then, the samples were transferred to artificial seawater (ASW) for 2 h before the start of the bioassay. A volume of 30 mL of the cell suspension (1×10^4 cells/mL) was added to each culture dish containing a glass microscope sample. The samples were rinsed with ASW gently after 8 days to remove cells that had not attached and were then treated with 5 mL of acetone for 15 min. The resulting eluate was measured for chlorophyll content with a UV spectrophotometer (760CRT double-beam ultraviolet–visible spectrophotometer).

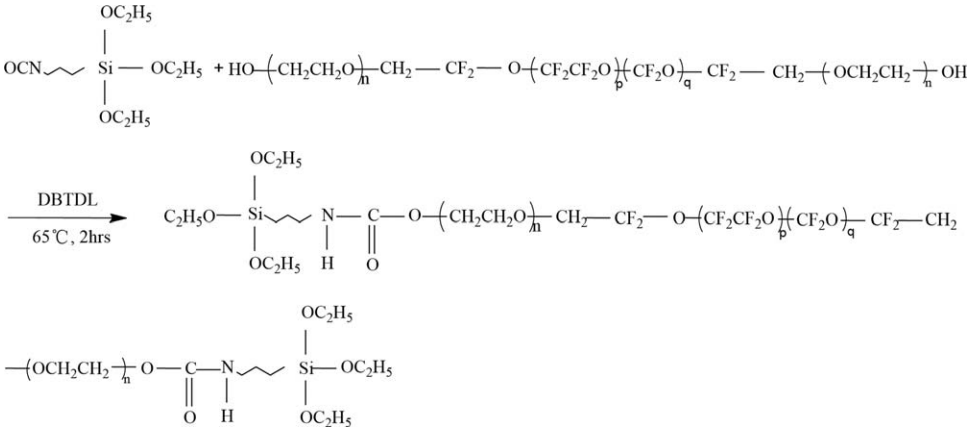

Scheme 2. Reaction scheme for the synthesis of the α,ω-triethoxysilane terminated PFPE oligomer PFU.

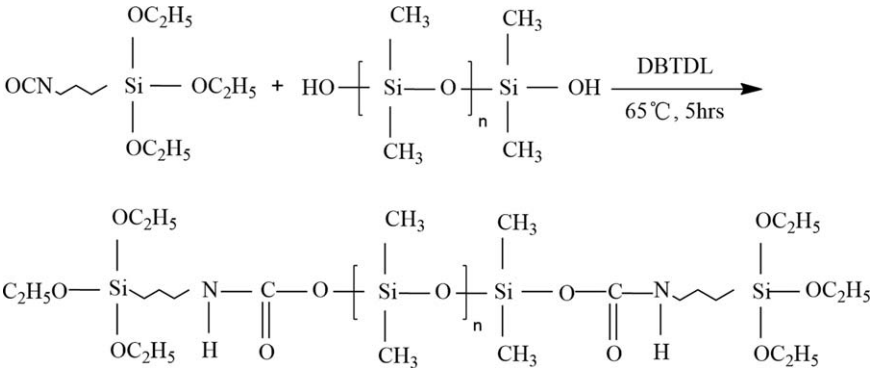

Scheme 3. Reaction scheme for the synthesis of the α,ω-triethoxysilane terminated PDMS oligomer TSU.

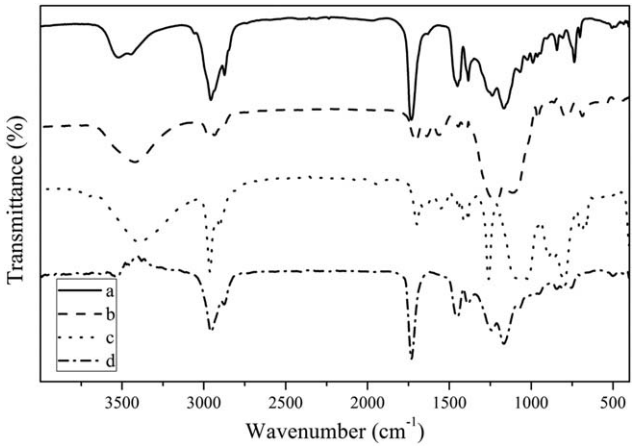

Figure 1. FTIR spectra of (a) acrylic polyols (AOH), (b) α,ω-triethoxysilane terminated PFPE oligomer PFU, (c) α,ω-triethoxysilane terminated PDMS oligomer TSU, and (d) TFS–AOH–B5.

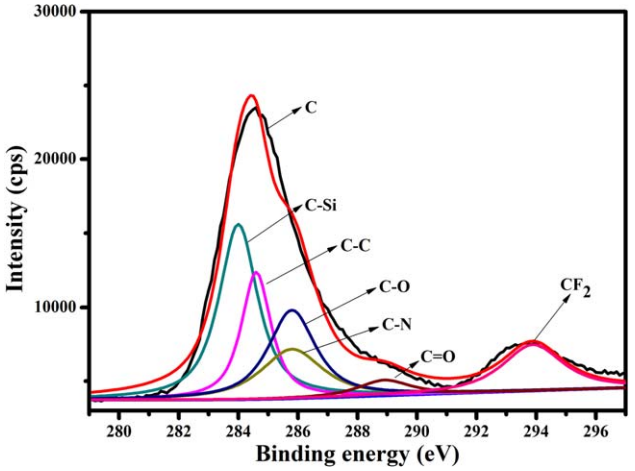

Figure 3. XPS C1s spectra of the polymer coating TFS–AOH–B5. [Color figure can be viewed in the online issue, which is available at wileyonlinelibrary.com.]

RESULTS AND DISCUSSION

Oligomer Synthesis

In this study, our focus was to develop coatings with an effective fouling releasing ability and good adhesion to the substrate for marine fouling-release applications. The strategy was to prepare a series of crosslinked network coatings based on PFPE/PDMS/acrylic polyols by a condensation reaction; this combines the advantage of fluorinated segments and a silicon component and simultaneously brought in an active group, such as siloxane functional groups. The specific synthetic processes of acrylic polyols, α,ω-triethoxysilane terminated PFPE oligomer, and α,ω-triethoxysilane terminated PDMS oligomer are shown in Schemes 1, 2, and 3, respectively.

In the presence of the radical initiator AIBN, the radical copolymerization of BA, MMA, and HEMA was accomplished, as shown in Scheme 1. During the process of the addition reaction in both Schemes 2 and 3, it was necessary to drop 3-fsisocyanatopropyltriethoxysilane and DBTDL slowly to ensure sufficient reaction and to prevent sudden polymerization.

The chemical structure of AOH, PFU, TSU, and the crosslinked network coating TFS–AOH–B5 (shown in Table I) were characterized by FTIR analyses. The FTIR spectra are presented in Figure 1. In the IR spectra of the acrylic polyols, the broad absorption band at 3424 cm^{-1} were attributed to stretching vibrations involving the —OH groups. The characteristic absorption peaks at 1635 cm^{-1} were ascribed to the disappearance of C=C. This suggested that the polymerization reaction occurred among acrylate monomers and —OH was accordingly incorporated into the side chain of AOH. In the IR spectrum of the oligomer PFU, in addition to the asymmetric stretching absorption peaks at 2934 cm^{-1} ($—CH_2$) and asymmetric stretching absorption peaks at 2978 cm^{-1} ($—CH_3$), there were also characteristic absorption bands of C—F bonds in the region 1150–1225 cm^{-1} for oligomer PFU. The disappearance of the characteristic absorption peaks of isocyanate group (2272 cm^{-1}) suggested that the addition reaction was complete in the synthesis of the oligomer PFU. The situation was the same as in the synthesis of the α,ω-triethoxysilane terminated PDMS oligomer. Meanwhile, the characteristic stretching vibration absorption twin peaks of the Si—O—Si bonds in the region 1024–1106 cm^{-1} and absorption bands of $Si—(CH_3)_2$

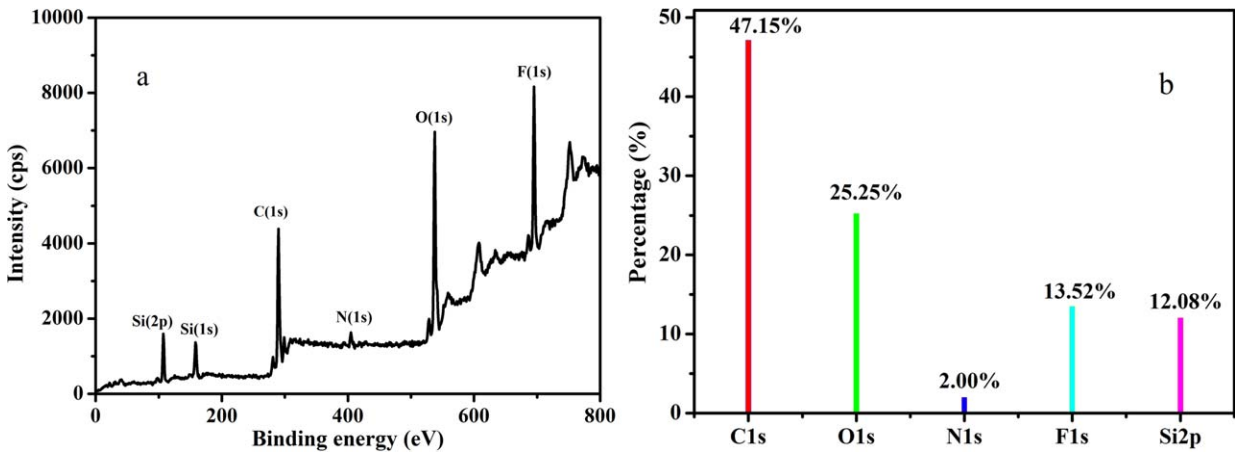

Figure 2. (a) Survey spectra and (b) elemental content analysis of the polymer coating TFS–AOH–B5. [Color figure can be viewed in the online issue, which is available at wileyonlinelibrary.com.]

Table II. XPS Atomic Surface Concentrations of the TFS–AOH–B Coatings

Coating	C (%)	O (%)	N (%)	F (%)	Si (%)
TFS-AOH-B1	58.99	24.72	0.77	8.49	7.03
TFS-AOH-B4	48.74	23.63	1.89	14.02	11.72
TFS-AOH-B5	47.15	25.25	2.00	13.52	12.08

(798 cm^{-1}) were observed for α,ω-triethoxysilane terminated PDMS oligomer. For a crosslinked network coatings, typically TFS–AOH–B5, the weakened absorption bands of —OH (3535 and 3449 cm^{-1}) demonstrated that there was a condensation reaction.

XPS Analysis

To further analyze the surface chemical structure of the coating, an X-ray photoelectron spectrometer was used. Figure 2 shows the survey scan spectra and elemental content analysis of the crosslinked network coating sample TFS–AOH–B5. The peaks were observed in the survey spectra at 690, 535, 400, 285, 168, and 102 eV because of fluorine (1s), oxygen (1s), nitrogen (1s), carbon (1s), silicon (2s), and silicon (2p), respectively. The atomic percentages of fluorine, oxygen, nitrogen, carbon, and silicon were 13.52, 25.25, 2.00, 47.15, and 12.08%, respectively. Figure 3 depicts the XPS C1s spectra of the TFS–AOH–B5 surface. The distinct C═O, C—O, C—N, and C—C peaks were observed at binding energies of about 289, 286, 286, and 285 eV, respectively. In addition, the expected CF_2 and C—Si peaks were found at binding energies of about 292 and 284 eV, respectively. The elemental analysis data of TFS–AOH–B1, TFS–AOH–B4, and TFS–AOH–B5 are summarized in Table II. For the ideal homogeneous coatings, TFS–AOH–B1, TFS–AOH–B4, and TFS–AOH–B5, both of the expected theoretical F and Si weight percentages should have been less than 2, 8, and 10%, respectively, according to Table I. Although for the TFS–AOH–B1, TFS–AOH–B4, and TFS–AOH–B5 surfaces, the experimental values of the F weight percentage calculated according to the data in Table II were 10.96, 16.82, and 16.13%, respectively. Simultaneously, the experimental values of the Si weight percentages calculated according to the data in Table II were 13.37, 20.72, and 21.23%; these were larger than the theoretical values. The results demonstrate that the side chains containing fluorine or silicon moved to the surface. Although the functional groups containing F or Si were difficult to remove from the crosslinked network coatings, thanks to the covalent bonds, there was an enrichment of F and Si at the surface in the respective coatings.

Table III. T_f, T_e, and T_g Values of the Crosslinked Network Coatings (TFS–AOH–B) and Acrylic Polyols

Sample	T_f (°C)	T_e (°C)	T_g (°C)
AOH	−3.22	11.75	6.97
TFS-AOH-A1	−16.66	−1.31	−8.74
TFS-AOH-A2	−14.77	−1.76	−8.63
TFS-AOH-A3	−12.34	1.46	−3.43
TFS-AOH-A4	−6.18	10.11	1.91
TFS-AOH-B1	−10.08	6.01	−0.86
TFS-AOH-B2	−12.72	1.44	−3.46
TFS-AOH-B3	−13.65	3.52	−1.8
TFS-AOH-B4	−13.51	2.65	−5.27
TFS-AOH-B5	−13.95	0.43	−6.33

DSC Analysis

The effects of the contents of the functional oligomers, PFU and TSU, on the glass-transition temperature of crosslinked network coating materials were systematically investigated.

First, when the total weight percentage of PFU and TSU was maintained at 16%, the DSC curves of the crosslinked network coatings TFS–AOH–A series (sample TFS-AOH-A1, TFS-AOH-A2, TFS-AOH-A3, TFS-AOH-A4 and TFS-AOH-A5 in Table I) and acrylic polyols were obtained, as shown in Figure 4. The details of the results about T_f (the starting points of the glass transition range), T_e (the ending points of the glass transition range) and T_g (the glass transition temperature) are presented in Table III. The glass-transition temperature of TFS–AOH–A was lower than that of AOH (6.97°C). As the weight percentage of PFU increased from 2 to 14%, the glass-transition temperature increased from −8.74 to 1.91°C. This illustrated that the effects of the contents of the functional oligomers, PFU and TSU, on the glass-transition temperature

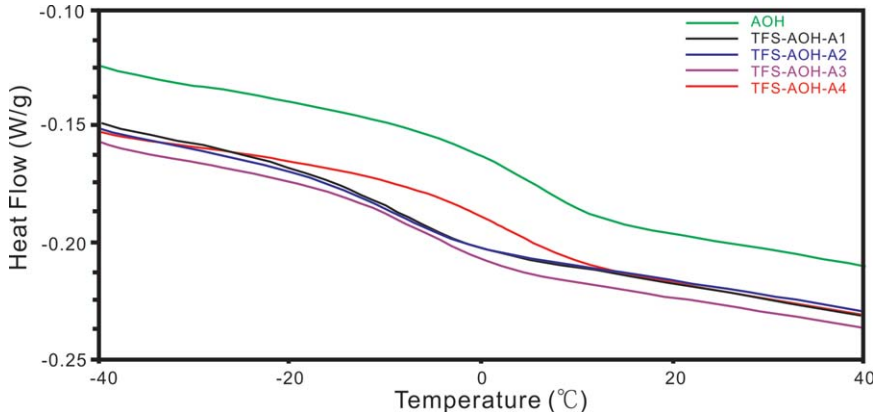

Figure 4. DSC curves of the crosslinked network coatings (TFS–AOH–A) and acrylic polyols. [Color figure can be viewed in the online issue, which is available at wileyonlinelibrary.com.]

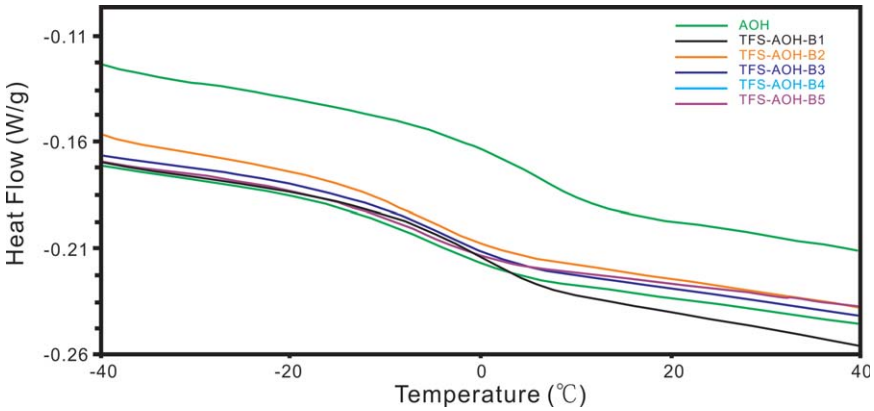

Figure 5. DSC curves of the crosslinked network coatings (TFS–AOH–B) and acrylic polyols. [Color figure can be viewed in the online issue, which is available at wileyonlinelibrary.com.]

Table IV. Test Liquids and Their Surface Energy Components

Surface energy data (mJ/m^2)	γ_{LV} (mJ/m^2)	γ_{LV}^p (mJ/m^2)	γ_{LV}^d (mJ/m^2)
Water	72.8	50.8	21.8
MI	50.8	0	50.8

Table V. θs and Surface Energies of TFS–AOH Films

Film	Water θ (°)	MI θ (°)	Surface energy (mJ/m^2)
AOH	85.1 ± 1.5	46.2 ± 0.8	38.8
DC 3140	112.8 ± 2.8	76.4 ± 2.1	19.4
TFS-AOH-B1	102.4 ± 0.8	74.1 ± 1.1	21.7
TFS-AOH-B2	102.2 ± 1.2	78.8 ± 1.2	19.6
TFS-AOH-B3	105.4 ± 1.4	77.4 ± 0.6	19.6
TFS-AOH-B4	107.8 ± 0.6	77.5 ± 0.5	19.3
TFS-AOH-B5	107.3 ± 0.5	76.1 ± 0.6	20.0

of the crosslinked network coatings materials were different. As the weight percentage of TSU increased, the glass-transition temperature decreased. Although the weight percentage of PFU increased, the glass-transition temperature increased. In addition, the effect of TSU on the glass-transition temperature of the coating materials was greater than that of PFU.

Table VI. Elastic Modulus and $(E\gamma c)^{1/2}$ Values of the TFS–AOH Films and Acrylic Polyols

Sample	E (MPa)	$(E\gamma c)^{1/2}$
AOH	104.73	63.78
DC 3140	308.72	77.39
TFS-AOH-B1	47.49	32.10
TFS-AOH-B2	38.70	27.54
TFS-AOH-B3	37.67	27.17
TFS-AOH-B4	22.16	20.68
TFS-AOH-B5	19.91	19.95

Second, when the weight ratio of PFU and TSU was maintained at 1, the DSC curves of the crosslinked network coatings TFS–AOH–B and acrylic polyols results are shown in Figure 5. The glass-transition temperature decreased from −0.86 to −6.33°C when the total weight percentage of PFU and TSU increased from 4 to 20%; this was lower than that of AOH. This demonstrated that the glass-transition temperature decreased as the total weight percentage of PFU and TSU increased.

Contact-Angle Measurements and Surface Energy Calculations

The surface free energy of the coating was calculated by the measurement of θ with two different probe liquids (water and MI) with known surface tensions[22] (as shown in Table IV) according to the Owens–Wendt method [eqs. (1) and (2)]:[20]

$$\gamma_{LV}(1+\cos\theta)=2(\gamma_{SV}^d\gamma_{LV}^d)^{1/2}+2(\gamma_{SV}^p\gamma_{LV}^p)^{1/2} \quad (1)$$

$$\gamma_{SV}=\gamma_{SV}^p+\gamma_{SV}^d \quad (2)$$

where the superscripts d and p are the dispersion and polar components of surface free energy, respectively; γ_{LV} and γ_{SV} are the interfacial tensions at liquid–vapor and solid–vapor interfaces, respectively; and θ is the static contact angle at solid–liquid–vapor interfaces.

The static θs and surface free energy of the coatings are listed in Table V. It was obvious that the surface free energies of the TFS–AOH films were lower than those of AOH (38.8 mJ/m^2) because of the incorporation of both the siloxane and fluorinated moieties. When the total weight percentage of α,ω-triethoxysilane terminated PFPE oligomer and α,ω-triethoxysilane terminated PDMS oligomer increased from 4 to 20%, the surface free energy decreased from 21.7 to 19.3 mJ/m^2. The low surface energy was mainly caused by the enrichment of F and Si on the coating surface.

Mechanical Properties of the Coatings

According to Kendall model,[23] the fracture or removal processes are influenced not only by the surface energy of the coatings but also by the modulus parameter (E) of the material.[24] The release force scales linearly with the cumulative elastic modulus and surface energy, that is, $(E\gamma c)^{1/2}$. The elastic modulus and $(E\gamma c)^{1/2}$ of the coatings are listed in Table VI. When the total weight percentage of the α,ω-triethoxysilane terminated PFPE oligomer and α,ω-triethoxysilane terminated PDMS oligomer increased from 4

Table VII. Adhesion and Antiseawater Immersion Performance of the TFS–AOH Films and Acrylic Polyols

Sample	Adhesion (grade)	Antiseawater immersion (after 21 days)
AOH	4B	Gloss loss
TFS-AOH-B1	5B	No change
TFS-AOH-B2	5B	No change
TFS-AOH-B3	5B	No change
TFS-AOH-B4	5B	No change
TFS-AOH-B5	5B	No change

to 20%, the elastic modulus of the coatings decreased from 47.49 to 19.19 MPa; this was also much lower than that of acrylic polyols named AOH. When the weight percentage was added to 16%, the increasing trend slowed down. The results demonstrated that both a low surface energy and low elastic modulus were achieved with an appropriate weight percentage of PFU and TSU. As shown in Table VI, as the total weight percentage of oligomer increased, the $(E\gamma c)^{1/2}$ value of the TFS–AOH–B samples decreased from 32.10 to 19.95; this was notably lower than those of AOH (63.78) and DC 3140 (77.39). The result indicates that the antibiofouling properties of the coatings were improved when more functional oligomer was brought in.

Adhesion and Antiseawater Immersion of the Film

The adhesion and antiseawater immersion performance are summarized in Table VII. As shown in Table VII, the adhesion of the crosslinked network coatings (TFS–AOH–B) on glass substrates were all scored as 5B. From the results, it was clear that all of the crosslinked network coating materials exhibited excellent adhesion on glass substrates, thanks to the siloxane functional group. Additionally, after 21 days of immersion in artificial seawater, all of the crosslinked network coatings basically maintained no change, and this demonstrated that these coatings exhibited good antiseawater immersion performance.

Biofouling Assays

Because bacterial adhesion on surfaces is a prerequisite for further biofouling caused by marine organisms,[25,26] it is very necessary to prevent and reduce the adhesion of bacterial. Figure 6 shows the numbers of bacterial cell colonies attached to the TFS–AOH–B-, AOH-, and DC 3140 coated glass slides and bare glass slide. We observed there were high-density bacterial cell colonies on the bare glass slide and DC 3140 and AOH-coated slides. On the contrary, only few bacterial cell colonies were found on the set of the TFS–AOH–B-coated slides after exposure to cultures of *E. coli* for

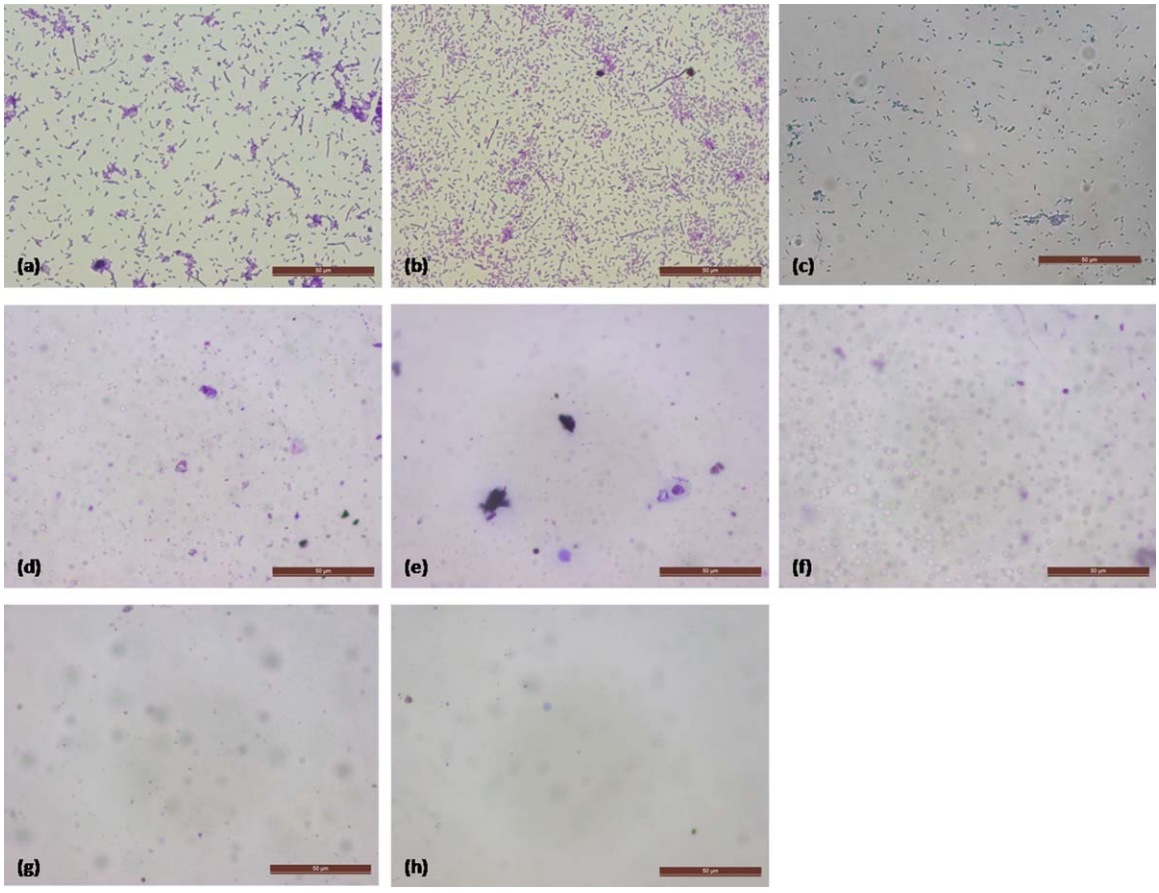

Figure 6. Optical microscopy images (500×) of the *E. coli* colonies after 24 h of exposure: (a) bare glass slide, (b) DC 3140 coated slide, (c) AOH-coated slide, (d) TFS–AOH–B1-coated slide, (e) TFS–AOH–B2-coated slide, (f) TFS–AOH–B3-coated slide, (g) TFS–AOH–B4-coated slide, and (h) TFS–AOH–B5-coated slide. [Color figure can be viewed in the online issue, which is available at wileyonlinelibrary.com.]

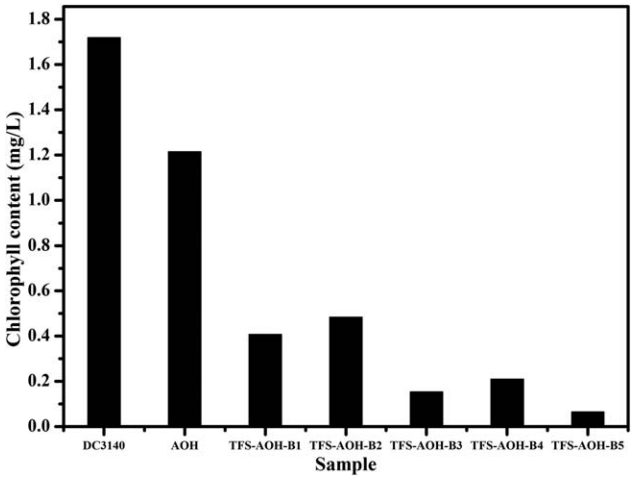

Figure 7. Chlorophyll contents of a bare glass slide, a DC 3140 polymer treated slide, an AOH oligomer treated slide, and TFS–AOH–B polymer treated slides.

24 h. It was obvious that the surfaces of the crosslinked network coatings incorporating both siloxane and fluorinated moieties possessed good resistance to the colonization of *E. coli*. We concluded that the numbers of bacterial cell colonies attached to the surfaces decreased with a lower surface energy and $(E\gamma c)^{1/2}$, which was aligned with Thorpe *et al*.'s results.[21]

According to the Beer–Lambert law and tricolor principle, the chlorophyll content on the sample surfaces was measured by a UV spectrophotometer. The results are shown in Figure 7. We found that the chlorophyll contents on AOH polymer-coated slide, DC 3140 coated slide and bare glass slide were 1.21, 1.72, and 0.60 mg/L, respectively; these values were larger than those on the TFS–AOH–B-coated slides (TFS–AOH–B1 = 0.41 mg/L, TFS–AOH–B2 = 0.48 mg/L, TFS–AOH–B3 = 0.15 mg/L, TFS–AOH–B4 = 0.21 mg/L, TFS–AOH–B5 = 0.06 mg/L). The results suggest that the crosslinked network coatings based on PFPE/PDMS/acrylic polyols had better antifouling performance than the acrylic polyol AOH, commercially available DC 3140, and bare glass slide. Meanwhile, the lower chlorophyll contents for the samples TFS–AOH–B3, TFS–AOH–B4 and TFS–AOH–B5 outlined in Figure 7 demonstrate that the antifouling performance of the coatings was enhanced by the incorporation of more siloxane and fluorinated moieties; this caused the lower surface energy, elasticity modulus, and lower $(E\gamma c)^{1/2}$ value.

CONCLUSIONS

Crosslinked network coatings based on PFPE/PDMS/acrylic polyols for marine fouling-release applications were prepared. The series of crosslinked network coatings based on PFPE/PDMS/acrylic polyols possessed good adhesion, antiseawater immersion performance, low surface energy, and low elastic modulus. Further biofouling assay investigation indicated that the series of crosslinked network coatings had better antifouling performance than the commercially available DC 3140 and bare glass slide.

ACKNOWLEDGMENTS

X.S. designed and supervised the research. F.Z. performed the majority of the experiments and wrote the article. Y.C., Z.C., Y.S., and N.L. performed the bacterial attachment experiment, the diatom Navicula settlement experiment, the differential scanning calorimetry experiment, and the X-ray photoelectron spectroscopy experiment, respectively. D.S. assisted with the writing of the article (especially image preparation). L.J., J.H., and L.S. contributed insightful discussions.

The authors thank the National Natural Science Foundation of China (contract grant number 51303102), the Professional and Technical Service Platform for Designing and Manufacturing of Advanced Composite Materials (Shanghai), the Shanghai Municipal Science and Technology Commission (contract grant number 13DZ2292100), and the Baoshan District Science and Technology Commission of Shanghai (contract grant number bkw2013142) for their financial support.

REFERENCES

1. Townsin, R. L. *Biofouling* **2003**, *19*, 9.
2. Schultz, M. P.; Bendick, J. A.; Holm, E. R.; Hertel, W. M. *Biofouling* **2011**, *27*, 87.
3. Lejars, M.; Margaillan, A.; Bressy, C. *Chem. Rev.* **2012**, *112*, 4347.
4. Clark, E. A.; Sterritt, R. M.; Lester, J. N. *Environ. Sci. Technol.* **1988**, *22*, 600.
5. Schultz, M. P.; Kavanagh, C. J.; Swain, G. W. *Biofouling* **1999**, *13*, 323.
6. Brady, R. F. *Defence Sci. J.* **2005**, *55*, 75.
7. Brady, R. F.; Singer, I. L. *Biofouling* **2000**, *15*, 73.
8. Kavanagh, C. J.; Quinn, R. D.; Swain, G. W. *J. Adhes.* **2005**, *81*, 843.
9. Terlizzi, A.; Conte, E.; Zupo, V.; Mazzella, L. *Biofouling* **2000**, *15*, 327.
10. Nendza, M. *Mar. Pollut. Bull.* **2007**, *54*, 1190.
11. Cassé, F.; Stafslien, S. J.; Bahr, J. A.; Daniels, J.; Finlay, J. A.; Callow, J. A.; Callow, M. E. *Biofouling* **2007**, *23*, 121.
12. DeSimone, J. M.; Williams, M. S.; Portnow, L.; Wood, C.; Zhou, Z.; Baucom, E.; Rothrock, G. D. WIPO Pat. WO/2007/025293 **2007**.
13. Krishnan, S.; Wang, N.; Ober, C. K.; Finlay, J. A.; Callow, M. E.; Callow, J. A.; Hexemer, A.; Sohn, K. E.; Kramer, E. J.; Fischer, D. A. *Biomacromolecules* **2006**, *7*, 1449.
14. Grunlan, M. A.; Lee, N. S.; Mansfeld, F.; Kus, E.; Finlay, J. A.; Callow, J. A.; Callow, M. E.; Weber, W. P. *J. Polym. Sci. Part A: Polym. Chem.* **2006**, *44*, 2551.
15. Kishita, H.; Sato, S. U.S. Pat. 20100272910, **2010**.
16. Mielczarski, J. A.; Mielczarski, E.; Galli, G.; Morelli, A.; Martinelli, E.; Chiellini, E. *Langmuir* **2010**, *26*, 2871.
17. Marabotti, I.; Morelli, A.; Orsini, L. M.; Martinelli, E.; Galli, G.; Chiellini, E.; Lien, E. M.; Pettitt, M. E.; Callow, M. E.; Callow, J. A.; Conlan, S. L.; Mutton, R. J.; Clare, A. S.; Kocijan, A.; Donik, C.; Jenko, M. *Biofouling* **2009**, *25*, 481.
18. Mera, A. E.; Wynne, K. J. U.S. Pat. 6265515, **2001**.
19. Sun, X. Y.; Su, Y. Q.; Jin, L. J.; Hang, J. Z.; Shi, L. Y. *Acta Polym. Sin.* **2013**, *1*, 134.
20. Owens, D. K.; Wendt, R. C. *J. Appl. Polym. Sci.* **1969**, *13*, 1743.

21. Thorpe, A.; Peters, V.; Smith, J. R.; Nevell, T. G.; Tsibouklis, J. *J. Fluorine Chem.* **2000**, *104*, 37.
22. Zhao, Q.; Liu, Y.; Wang, C.; Wang, S.; Muller-Steinhagen, H. *Chem. Eng. Sci.* **2005**, *60*, 4858.
23. Kendall, K. J. *J. Phys. D* **1971**, *4*, 118.
24. Singer, I. L.; Kohl, J. G.; Patterson, M. *Biofouling* **2000**, *16*, 301.
25. Chambers, L. D.; Stokes, K. R.; Walsh, F. C.; Wood, R. J. K. *Surf. Coat. Technol.* **2006**, *201*, 3642.
26. Feng, S. J.; Wang, Q.; Gao, Y.; Huang, Y. G.; Qing, F. L. *J. Appl. Polym. Sci.* **2009**, *114*, 2071.